

Anticipating the Limits of Climate Adaptation: Evidence from U.S. Irrigation Adoption

Aime Bierdel*

This version: January 2025

Abstract

Will technology help us adapt to future climate conditions? We examine irrigation—an essential technology for adapting agriculture to climate change—and find a “hump-shaped” adoption pattern: irrigation use increases at mild dryness levels and declines under severe dryness despite increasing benefits and willingness to pay for irrigated land. We provide evidence that water scarcity, itself worsened by climate change, drives these dynamics by limiting the effectiveness of irrigation technologies and their adoption in the United States. This “window of opportunity” pattern—where adaptation technologies are most effective under moderate climate change and lose effectiveness thereafter—holds true for many climate adaptation strategies. Incorporating this feature into a stylized macro-finance model yields diverging adaptation strategies at different levels of global warming: adaptation investment is high for moderate global warming and low for severe warming. Hence uncertainty about future climate discourages adaptation investment by making its returns uncertain. Our results highlight the benefits of commitment mechanisms that can reduce climate uncertainty as they encourage more proactive adaptation efforts.

*ab4884@columbia.edu

1 Introduction

The early climate economics literature established that our collective effort to reduce greenhouse gas emissions should be sized by an inter-temporal trade-off: the future welfare costs of climate change against the immediate cost of its prevention. Turning these insights into actionable policy has since hinged on our ability to predict and quantify the welfare damages climate change will cause. To tackle this challenge, economists have developed increasingly complex integrated assessment models building on the seminal work of William Nordhaus (1992) (20). The premise of these models is to incorporate both endogenous climate change dynamics and endogenous adaptation of economic agents while allowing for a large variety of channels through which climate impacts economic activity. Hence understanding the opportunities and limits of adaptation to climate change is a crucial endeavor for economists and policymakers.

In this paper, we focus on adaptation of the agricultural sector to dryness. Agriculture is among the sectors most affected by climate change as its output is physically determined by local weather conditions and water supply. The sector still employs more than 50 % of the population in South Asia and Sub-Saharan Africa¹, making its adaptation an important challenge for the developing world. The future of agriculture in areas set to become significantly dryer depends on the implementation of a series of adaptations such as increased water efficiency, crop adaptation through selection or genetic modification, innovative farming methods or irrigation. We study the installation of irrigation systems as an example of adaptation technology. It is a natural choice as irrigation techniques have been adopted at scale for decades to insulate farmers from precipitation variability and therefore offer a long track record of benefits and adoption to study.

In the first section, we document several key facts about irrigation adoption patterns in U.S. agriculture from 1997 to 2022. The main one is visible on Figure 1, which shows the evolution the log of irrigated surfaces and the estimated trend in the DSCI drought index² in the US over the period. Irrigation is progressing in the Eastern and Central regions where dryness evolution is mild and scaling back on a significant portion of the Western regions where dryness severely worsened. This first finding is counter-intuitive as one would expect adoption to be strictly increasing with dryness, and motivates the rest of this paper.

¹FAO & World Bank <https://www.fao.org/4/i2490e/i2490e01b.pdf>

²A measure of dryness. A detailed presentation of this quantity is given in the first section

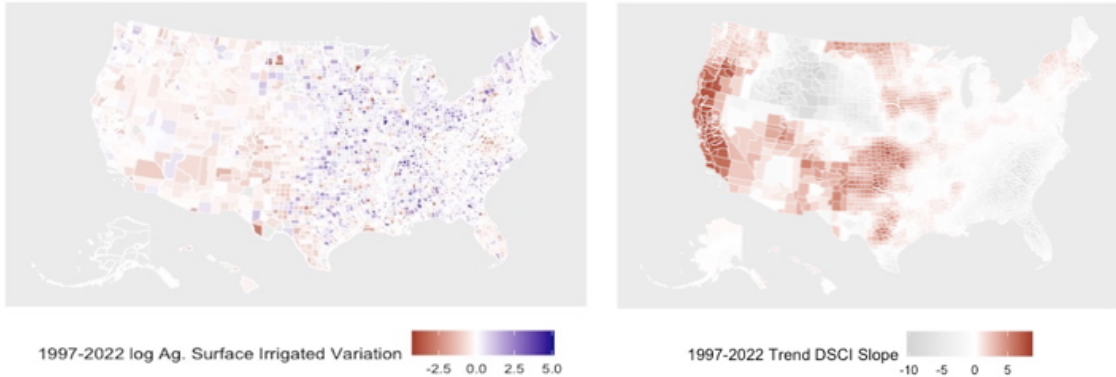


Figure 1: Evolution of irrigated surfaces and estimated DSCI trend over 1997-2022

We start by showing that this pattern holds true under rigorous statistical analysis. To do so, we exploit cross-sectional differences in trend dryness between US counties to identify the resulting irrigation adoption variations through panel fixed effect regressions. Second, we use county-level data on agricultural rents to construct a measure of farmers’ willingness to pay for irrigation. As expected, we find that it is strictly increasing in dryness, showing that adoption of the technology would progress if it could. Third we use cross-sectional differences in local water resource endowments to show evidence that water scarcity - itself worsened by climate change - is driving the decrease in adoption.

In the second section, we construct a partial equilibrium model of irrigation investment where dryness has two effects. On the one hand, it lowers agricultural productivity and on the other hand it depletes local water resources, increasing the cost of running irrigation systems. While the technology successfully mitigates damages from dryness, it does so at an increasing cost as droughts become more severe. The model successfully replicates the three facts observed in the data under the condition that water extraction costs increase faster than irrigation benefits as dryness increases. Satisfying this condition implies that irrigation as an adaptation technology has hump-shaped returns: high at mild dryness levels where water resources are plentiful and low at severe dryness levels where local water resources are depleted. We show that this technological property can be straight-forwardly aggregated, so that a social planner deciding levels of adaptation spending at the macroeconomic level would face a marginal return to adaptation investment that is hump shaped with respect to climate change.

Finally, we incorporate this technological constraint in a stylized climate macro-finance model featuring adaptation investment in the spirit of Hong et al.(2020)

(16). It generates adaptation investment patterns similar to the ones observed for irrigation (high investment at intermediate dryness levels, low investment at high dryness levels). With this realistic technological constraint, including adaptation into integrated assessment models delivers an improvement in the social cost of carbon relative to the no adaptation benchmark for moderate/optimistic climate change scenarios only. Most importantly, our findings lead to the conclusion that optimal adaptation strategies at mild and severe climate change scenarios are opposite. As a consequence uncertainty surrounding future climate conditions discourages adaptation investment as it increases the unpredictability of its returns. In other words, technological adaptation suffers from inertia and does not provide insurance against the worst climate scenarios. Assuming that our findings generalize to the broader set of technologies available, technological adaptation represents a window of opportunity at most. This reinforces the need for strong commitment mechanisms that reduce uncertainty about future climate as it directly influences economic incentives to adapt.

Related literature This study contributes to a nascent empirical literature that studies adaptation through the lens of currently available technologies. This recent effort complements the large empirical literature that provides quantification of climate-related damages to calibrate integrated assessment models.(Addoum & al. 2020 (1), Hsiang & Gina 2014 (17) , Boustan & al. 2020 (7)...). This literature leverages past weather realizations to measure economic damages from extreme climatic events and other consequences of climate change. However it does not address agents' capacity to adapt, which has since been the direction of development for integrated assessment models. To answer this shortcoming, several studies have been explicitly focusing on specific adaptation technologies and their trade-offs. Benetton & al. (2023) (4) study the impact of adaptation investment by focusing on a seawall recently built in Venice. Hong & al. 2021 (16) quantify the benefits of protection against Hurricanes. Aker & al. (2021) study environmental technology adoption in Sahel (2), Taylor (2023) (25) also studies irrigation through its impact on water demand and other externalities. Our findings also align with Giesecke & al. (2022) (12) who find significant negative impacts of water scarcity on agricultural land prices in California, while we focus on the impact on rents.

Second we contribute to advancing the modeling of adaptation in the context of integrated assessment models. Adaptation to climate change can take two distinct forms: technological adaptation (reducing damages or finding ways to make production resilient to the future climate) and spatial adaptation (migrations and relocation

of economic activity in order to escape the most vulnerable areas). The recent climate macroeconomic literature has mainly focused on incorporating and modeling the latter by borrowing the tools from the spatial economics literature (Cruz & al. 2021 (9), Desmet & al. 2021 (11), Conte & al. 2020 (8), Bilal & Rossi-Hansberg (6), Rudik & al. (2022) (24)). However there has been little work on the role played by technological adaptation. We contribute by discussing the generalization of our empirical findings to calibrate the marginal product of technological adaptation at the macroeconomic level.

Finally we contribute to the theoretical climate finance literature by highlighting a new interaction between uncertainty and adaptation to climate change. In the literature, several papers have addressed some aspects of the interaction between climate change uncertainty and adaptation. Rudik (2020) (23) discusses the uncertainty of damage estimates and optimal climate policy. Hong & al. (2020) (16) show that with Bayesian belief formation about future disaster frequency, adaptation allows to reduce over-reaction to disasters and can play a role in mitigating the effects of uncertainty. In Guthrie (2019) (13), adaptation timing strategy is discussed in a context where uncertainty resolves gradually. In our framework, uncertainty is a detriment to adaptation as its inefficiency in extreme scenarios creates inertia and discourages anticipatory adaptation investment, a novel mechanism.

The paper is structured as follows. Section 2 presents our empirical results. Section 3 presents a stylized model that rationalizes our empirical findings at the microeconomic level, aggregates them into a macroeconomic adaptation function and derives its key properties. Section 4 presents a stylized macroeconomic model with climate change where the adaptation function's properties are inherited from the micro-foundations laid out in Section 3. We discuss the consequences of the properties of adaptation functions we uncovered for integrated assessment models and policy. Finally we conclude.

2 Adaptation through irrigation in U.S. agriculture

In this section, we will quantitatively show three facts about irrigation in U.S. agriculture over the period 1997-2022. First we show that the willingness to pay for irrigation systems measured using agricultural rent premia for irrigated land is strictly increasing in dryness, implying that this adaptation technology would be adopted at severe dryness levels if it could. Second we measure that despite a strictly increasing willingness to pay, adoption of irrigation systems has an inverse U shape

(“hump” shape) with respect to dryness: it increases at mild levels and decreases when dryness becomes severe. Finally we show that the decline in adoption is only present where local water resources are highly stressed, making the use of irrigation systems impossible and explaining the hump shaped pattern observed.

2.1 Data

Measuring dryness We use the Drought Severity and Coverage Index (DSCI) from the U.S drought monitor as our favored measure of dryness. It offers the advantage of spatial granularity (county-level measure) and is a blend of technical indicators and expert opinions that make it more robust than alternatives relying exclusively on remote-sensing or weather-related measures. In particular, it incorporates assessments of soil moisture, a critical component of dryness for agriculture, making it the most suitable dryness index for our purposes. The measure is averaged at yearly frequency from 2000 to 2024. Its average trend over the period 1997-2022³ is shown in Figure 1 across the US. The index is an integer between 0 and 500, 500 denoting dryness of maximum intensity and 0 a suitable wetness level. Each tranche of 100 denotes a qualitatively different level of dryness ranging from none (0), abnormally dry (≤ 100), moderate ($[100, 200]$), severe ($[200, 300]$), extreme ($[300, 400]$) to exceptional ($[400, 500]$).

Water depletion index We obtain the water depletion index from the Aqueduct 4.0 database. The index is built from the simulations of a hydrological model which estimates local water supply and demand at the aquifer⁴ level. The size of aquifers varies greatly but most are at a sub-state geographic scale that makes this data suitable for a county-level analysis. Indeed substantial heterogeneity in the water depletion index exists at this level as shown on Figure 7. The index is computed as the ratio of water demand to total renewable water supply at the aquifer level. It is strictly greater than 0 and the larger, the more local water resources are strained. We projected the measure onto county geographic shapes by averaging the value of the index over the surface of each county. A supplementary benefit from using this measure is its availability as projections under different time horizons and climate forcing scenarios by the World Resource Institute and Aqueduct 4.0 (19).

³Our period of study for irrigation adoption. Construction of the trend is discussed later in the section. The trend over 1997-2002 is approximated to be the same as the trend over 2000-2002.

⁴Underground pocket of water that can be used for irrigation purposes

Census of Agriculture We use the census of agriculture, a survey conducted every 5 years in the US with a large number of sections ranging from farm demographics and practices to economic and physical variables. We extract from the survey three different series at the county level:

1. *Average cash rents*: The average cash rents paid by farmers who rent part or all of the land they exploit. The measure is expressed in dollar per acre and recorded yearly at the county level for the period 2007-2022. This measure is available for general cropland and irrigated cropland, allowing us to compute a county-level measure of irrigation premium discussed in Section 2.2.
2. *Irrigated and agricultural surfaces*: we obtain the county-level reports of number of acres used for cropland, pasture or other agricultural purposes (we define agricultural land as the sum of the three categories) and the number of irrigated acres for each county at the 5-year census frequency from 1997 to 2022. We also retrieve the number of farms in order to build a measure of average farm size that will be used a control in our regressions.

Data availability Figure 5 in the appendix shows the rent premium (the main dependent variable of our measurements presented in Section 2.2 and calculated from cash rents) in year 2022 across the US. This data availability reflects the one of cash rents. Despite missing observation in large subsets of the country, we observe rents in key locations for our analysis. The driest areas in the West have ample representation as well as the highly irrigated area around the Mississippi river. There is certainly non random selection to the missing values as less dry areas where irrigation is not widespread are more likely to be missing. Yet it is unlikely to meaningfully bias our analysis because it mostly affects estimates at very low levels of dryness where we expect willingness to pay for irrigation to be small. Conversely we have excellent representation in the driest and most irrigated areas where our quantification effort is focused. For irrigated and agricultural surfaces, some individual county x years are missing for anonymity purposes but more than 99% of the contiguous U.S. and years are available, giving us excellent coverage.

Economic controls In order to control for potential confounding factors, we retrieve yearly county-level GDP and unemployment rate from the bureau of economic analysis (21). The series are available since the start of the 2000s, allowing for complete coverage of our sample. These controls are an attempt to capture local economic factors that could be varying with dryness and are affecting economic decisions of

farmers. We discuss the validity of these controls in the identification discussions following each of our regressions below.

Descriptive statistics We present descriptive statistics for the main variables in Table 1.

Variable	Symbol	Mean	Std Dev.	p05	p95	Observations	Units
Irrigation Premium	R_{it}^{Irrig}	56	26	7	87	1893	%
DSCI	d_{it}	70	98	3	314	12180	—
Irrigation Share	s_{it}	6.7	13	0.3	35	13314	%
Irrigated Surface	S_{it}^{Ir}	2.0×10^4	5.4×10^4	2.3×10^1	1.1×10^5	14058	Acres
Agricultural Surface	S_{it}^{Ag}	2.6×10^5	3.6×10^5	1.4×10^4	8.7×10^5	14379	Acres
Water Depletion Index	$W_{i,t}^d$	0.062	0.577	0.003	1.112	15185	—

Table 1: Descriptive statistics for main variables

2.2 Irrigation Rent Premia

We now turn to the formal analysis of the premium on cash rents paid by farmers to operate irrigated land.

Construction of the rent premium Let $R_{i,t}^{IrrigatedCropland}$ and $R_{i,t}^{Cropland}$ be the average cash rents paid by farmers in county i and year t for irrigated and non irrigated cropland respectively. We construct the irrigation premium as:

$$P_{i,t}^{Irrig} = \frac{R_{i,t}^{IrrigatedCropland} - R_{i,t}^{Cropland}}{R_{i,t}^{IrrigatedCropland}} \quad (1)$$

Where $R_{i,t}^{IrrigatedCropland}$ is the average cash rent paid for irrigated cropland in county i at date t and $R_{i,t}^{Cropland}$ is the same measure for general cropland. We normalize by the rent of irrigated cropland as it should correspond to the owner’s share of the maximum surplus extractible from the land. We interpret this premium as reflecting the share of the total surplus from exploiting the land attributable to irrigation systems. Indeed, in a scenario where non-irrigated cropland has the same productivity as irrigated cropland (perfect wetness conditions), the cash rent of irrigated land should be equal to the rent of non irrigated land plus the cost of the irrigation infrastructure. The implied premium should be small and strictly positive (merely reflecting

higher infrastructure costs). Conversely in extreme scenarios where agriculture is barely possible without irrigation, the premium should be close to 1, reflecting that almost 100% of the surplus from farming the parcel is attributable to the presence of irrigation. We will also formally derive an expression for the theoretical counterpart to this quantity in Section 3.1.

Land Rental Market We chose to focus on rents for our analysis for several reasons. According to the USDA (10), 54% of all cropland and 28% of pastureland is rented while the remainder is owner-operated which suggests that the market is large enough to be representative of more general dynamics in U.S. agriculture. Among the possible lease contracts, fixed cash agreements corresponding to our observations represent more than 70% of all agreements. The second reason is the relatively high frequency of lease renewals, with 70% of agreements (57% of total rented surface) being renewed every year and more than 80% every three years. This ensures that rents are representative of current conditions rather than long term expectations, making them a better object of study than land prices for our purposes. Finally the rental market is largely a relationship market with little competitive entry (the supply of land is largely fixed) where the argument that rents reflect a negotiated split of the surplus is defensible. Note that this also bypasses one of the main difficulties that a study focused on crop yields would encounter: we can ignore heterogeneity in agricultural practices or underlying crops. We simply assume that the land is at its highest and best use and that the underlying practices are on average optimal for the parcel. The split of the surplus from farming measured through the rents is then, on average, the "optimal" surplus extractible from the land.

Extracting drought trends We want to quantify the marginal benefit to installing an irrigation system at different levels of dryness. We first regress our measure of dryness on time with an intercept for each county to estimate county-level trends over the 2000-2023 period where our dryness measure is available. This is similar to the trend extraction approach in Hong & al. (2019)(15). The specification is simply:

$$d_{i,t} = \beta_{0,i} + \beta_{1,i}t + \epsilon_{i,t} \quad (2)$$

Where $d_{i,t}$ is the 5 year averaged drought index. We extend the value of the trend over 2000-2002 to the period 1997-2000 in order to be able to fully utilize our irrigated surfaces sample that starts in 1997. We then use the values predicted for $d_{i,t}$ as our regressor in all following regressions (indicated by a bar \bar{d}_{it}). It represents the stable, trending component of dryness that should be reflected in the premium

farmers are willing to pay to rent irrigated land and is also a sensible statistic for decisions to adopt irrigation systems. Utilizing the trend rather than the value to estimate elasticities is also justified by the compounding effects of hydrological climate extremes described in Grogal & al. (2021) (14), suggesting that a measure that captures repeated and prolonged exposure should better capture the long run impacts of climate change.

Panel specification We choose a panel specification with a yearly time step and time/county-level fixed effects. Formally we estimate:

$$P_{it}^{Irrig} = r_0 \bar{d}_{i,t} \times \mathbb{1}\{\bar{d} \in [0, 100]\} + r_1 \bar{d}_{i,t} \times \mathbb{1}\{\bar{d} \in [100, 150]\} + r_2 \bar{d}_{i,t} \times \mathbb{1}\{\bar{d} \in [150, 200]\} + r_3 \bar{d}_{i,t} \times \mathbb{1}\{\bar{d} > 200\} + \alpha_i + \delta_t + \epsilon_{i,t} \quad (3)$$

And the pooled coefficient regression:

$$P_{it}^{Irrig} = r \bar{d}_{i,t} + \alpha_i + \delta_t + \epsilon_{i,t} \quad (4)$$

Where P^{Irrig} is defined in Equation 1, \bar{d}_{it} is the past 5 year average trend in dryness index (DSCI) in county i (standardized), (δ_t, α_i) are time and individual fixed effects respectively and ϵ_{it} is an i.i.d noise term. The regression covers the years 2007-2022 where the rents data is available. We estimate a pooled regression representing an average effect and four coefficients r_0, r_1, r_2 and r_3 for four groups: one having average drought trend inferior to 100, between 100 and 150, 150 and 200 (moderate) and above 200 (severe). This allows to identify the thresholds of dryness where the surplus from irrigation increases the most and to allow for a non linear relationship between the rent premium and dryness. No US county has an average value higher than 300, which would correspond to "extreme" in the US drought monitor specification. A quintile-binned scattered view of the relationship between the premium and our measure of dryness is shown in Figure 6 in the appendix. Visual inspection reveals a strongly increasing relationship which is confirmed by the regression results obtained below. The availability of a large number of counties in different geographies having faced different dryness conditions over the last 25 years gives both temporal and cross-sectional variation to our sample, which is our main argument for identification.

Estimation results Table 2 shows the results of the estimation for the pooled and the piece-wise estimators. Note that the values reflect the impact of an increase of the extracted trend by 1 standard deviation (≈ 45 DSCI units). It is our baseline estimate and reveals an increasing relationship for high enough levels of dryness. In

the group culminating above 200 of average trend DSCI over the period, an increase of DSCI by one standard deviation increases the irrigation premium by 20.1%. Putting this number in perspective, if we admit that the irrigation premium captures the surplus generated by irrigation as a proportion of the total surplus generated by farming, non irrigated land loses 20% of its productivity every 45 DSCI units in the 5 last years relative to non irrigated land at these levels of dryness. This quantifies the premium to irrigation as climate becomes dryer and also confirms that the returns to the technology are strictly increasing in dryness. Therefore the ambivalent adoption pattern visible in Figure 1 is not caused by inefficiency at severe dryness levels. We will show in the next section that adoption decreases *despite* these increasing returns because of an other consequence of dryness: water scarcity. Note that our finding of large effects visible only at the tail of the event distribution is shared by Albert & al. (2021) (3) who study the impacts of droughts in Brasil using a different dryness measure. An alternative quadratic specification shown in Table 5 of the appendix exhibits a similar pattern.

<i>Dependent variable:</i>		
Irrigation Premium		
	(1)	(2)
r	0.017*** (0.005)	
r_0		-0.024 (0.016)
r_1		0.0002 (0.006)
r_2		0.042*** (0.006)
r_3		0.201*** (0.010)
Observations	7,671	7,671
Effects	Time & County FE	Time & County FE

Note: *p<0.1; **p<0.05; ***p<0.01

Table 2: Irrigation premium regression results

Identification The identification argument for this regression is standard within the economic literature that estimates damage functions for climate-related events. Idiosyncratic differences between temporal variations of trend dryness over the sample period identify our coefficients rather than pure cross-sectional differences, which is in line with the objective to account for the effects of changing levels of dryness as climate change progresses. The fixed effect specification eliminates the risk of first order contamination by non time varying confounding factors, leaving only potential time-varying confounding factors that may be correlated with dryness. We add county-level controls (GDP, unemployment, average economic farm size and average farm size measured by surface) in order to account for pure demand-side and wealth-driven confounding factors. Indeed dryness is correlated with other climate-specific variables that impact the economy in a variety of ways. A dryer climate may be correlated with more general effects on labor productivity, depressing local demand and demand for agricultural goods, influencing the demand for agricultural land. The farm-specific characteristics help control for wealth effects and financial frictions that may explain differences in observed premia independently of the pure effect of dryness. The inclusion of these controls does not change our estimates meaningfully.

2.3 Evolution of Irrigated Surfaces

We confirmed that the premium farmers are willing to pay is strictly increasing in our measure of trend dryness and now turn back to the irrigation adoption pattern observed in the data. Given that the technology generates a higher return in drier regions, we would expect irrigated surfaces to progress more in drier regions absent any constraint on the deployment of the system. We turn to the formal confirmation that irrigation adoption is hump-shaped with respect to trend dryness and show evidence that this pattern is effectively due to local water scarcity constraints.

Dependent variable We want to understand what are the adoption patterns at different levels of dryness. We choose to focus on the log agricultural surface irrigated as our variable of interest. Since counties are heterogeneous in size and quantity of land available to agriculture, it is important for our specification to be immune to first order effects of scale. The presence of fixed effects and a log specification ensures that this is the case. We acknowledge that our measure of dryness only noisily captures real conditions and has no reason to produce linear impacts given that it is an aggregation of several categorical grades over a full year. Hence we opt for a piece-wise linear specification to obtain "local" derivatives (local marginal

effects) at different levels of long term dryness (corresponding to the long run effect of a warming climate). This is the rationale for running the estimation by bracket of values of average trend DSCI (\bar{d}) over our sample period 1997-2022.

Specification The panel fixed-effect specification we run is

$$\begin{aligned} \log(S_{it}^{Irrig}) = & a_1 \bar{d}_{i,t} \times \mathbb{1}\{\bar{d} \in [0, 50]\} + a_2 \bar{d}_{i,t} \times \mathbb{1}\{\bar{d} \in [50, 100]\} + \\ & a_3 \bar{d}_{i,t} \times \mathbb{1}\{\bar{d} \in [100, 150]\} + a_4 \bar{d}_{i,t} \times \mathbb{1}\{\bar{d} \in [150, 200]\} \\ & + a_5 \bar{d}_{i,t} \times \mathbb{1}\{\bar{d} \in [150, 200]\} + \alpha_i + \delta_t + \epsilon_{i,t} \end{aligned} \quad (5)$$

Where α_i, δ_t are the individual and time fixed effects respectively, $\bar{d}_{i,t}$ is the last 5 year averaged extracted time trend of the DSCI and \bar{d} is the average extracted DSCI time trend over the full sample years.

<i>Dependent variable:</i>	
log Irrigated Acres	
a_1	0.323***
$\bar{DSCI} \leq 50$	(0.103)
a_2	0.114***
$\bar{DSCI} \in [50, 100]$	(0.034)
a_3	-0.013
$\bar{DSCI} \in [100, 150]$	(0.018)
a_4	-0.046***
$\bar{DSCI} \in [150, 200]$	(0.017)
a_5	-0.766***
$\bar{DSCI} \geq 200$	(0.108)
Observations	14018
Effects	County & Year

Note: *p<0.1; **p<0.05; ***p<0.01

Table 3: Irrigation surface regression results

Estimation results We observe a humped-shaped adoption pattern, with sharply increasing surface irrigated below 100 trend average DSCI and decreasing above 150. This result is in agreement with the initial visual observation of increasing irrigation in counties with mild dryness levels and decreasing irrigation for the driest western

counties. It is likely that competition with other uses (households, industry, energy generation) for surface waters and exhaustion of some groundwater resources have started to challenge the extent to which irrigation can be implemented. Decreasing availability of water resources could challenge the increasing returns to the equipment by constraining its use. We confirm this inverse U shaped pattern by running a quadratic specification for robustness. The results are presented in Table 6 in the Appendix and confirm the findings from our main specification.

Identification The identification argument for this regression is in large part identical to section 2.2. Difference in within county temporal variations identify our coefficients. Time and individual fixed effects control for general macroeconomic factors and non time varying confounding factors that could obscure our results. The main argument solidifying the above results is the inclusion of local economic controls (GDP, unemployment) that can capture local land demand factors that may correlate with dryness. As other land uses depend on the local climate, it may dryness affects alternate land use options in addition to affecting farming returns. The value of alternative land uses should be strongly well captured by local economic activity and hence the local GDP/ unemployment measures present in our controls. Measures of farm size are an attempt to control for the effects of financial frictions or other effects that may prevent investment into irrigation despite being economical, although we acknowledge imperfectly.

Water scarcity To validate the hypothesis that water scarcity is linked to the decline in land irrigated, we use the water depletion index developed and distributed by the World Resource Institute. The index combines outputs from a hydrological model to represent the degree of depletion of local water resources (both ground and surface water). The index has no yearly time variation but is instead computed on an average period covering most of our sample (mid 1990s to 2014). Figure 7 shows the value of the index for the period. We observe visually that these areas are associated with large declines in irrigated surface, which will be confirmed by measurement. We run a fixed effects panel data regression with the following specification:

$$\log(S_{it}^{Irrig}) = b_0 + b_1 \bar{d}_{i,t \rightarrow t-5} + b_2 \bar{d}_{i,t \rightarrow t-5} \times bwd_i + \alpha_i + \delta_t + \epsilon_{i,t} \quad (6)$$

Where bwd is the base water depletion index for the current climate estimated by the World Resource Institute. The results shown in Table 4 demonstrate that in counties where water depletion is not a current problem (bwd close to 0), irrigated surface increases in reaction to an increase in the trend dryness. The interaction term between the trend dryness and the water depletion index is sharply negative,

indicating that the surface irrigated decreases only when water stress is high. While not a direct causality, this result strongly suggests that water depletion is the driver behind the hump-shaped irrigation adoption pattern. This has consequences for the returns to investing in the technology. The infrastructure may become unusable due to rising water availability problems, leading to low returns on investment due to decreasing expected utilization. We formalize this insight in the next section through the lens of the technology’s protection profile.

	<i>Dependent variable:</i>	
	log Irrigated Acres	
	(1)	(2)
b_1	0.054*** (0.166)	0.044*** (0.016)
$b_2 = b_1 \times bwd_i$	-0.079*** (0.013)	
$b_3 = b_1 \times \mathbb{1}\{bwd \geq 0.8\}$		-0.088*** (0.019)
Observations	7,671	7,671
Effects	Time & County FE	Time & County FE
<i>Note:</i>	*p<0.1; **p<0.05; ***p<0.01	

Table 4: Irrigation surface water depletion interaction regression results

Corroborating existing evidence Note that our findings are complementary to Albert & al. (2021) (3), who find that extreme droughts displace workers and capital away from agriculture and that losses are concentrated at the very tail of the distribution of events. Similarly in our data the premium for irrigated land (a measure of relative productivity from the investors’ perspective) skyrockets for very intense levels of dryness due in large part to a large decrease in non irrigated farmland rents.

Bridge to the theory To summarize, we have found that irrigation adoption is humped-shaped with respect to dryness. It increases at mild dryness levels and decreases beyond a certain level of intensity. We have shown that the willingness

to pay for irrigated land is strictly increasing in dryness, suggesting that adoption would be increasing if not constrained. Finally we have shown suggestive evidence that water scarcity - another phenomenon made worse by increasing dryness levels - is responsible for the decrease in irrigation adoption. In the next section, we propose a reduced form model of irrigation investment that rationalizes these findings under certain conditions.

3 Micro-foundation of macroeconomic adaptation functions

3.1 Microeconomic adaptation

We start this theoretical section by formalizing a parsimonious model of adaptation investment that rationalizes our empirical findings. In concrete terms, we show that if the cost of water extraction increases faster than farming returns decrease with dryness, then it is possible to obtain increasing irrigation rent premia and a hump shaped irrigation adoption pattern simultaneously. Finally will show that these conditions imply hump shaped returns to irrigation as an investment, a key property for the rest of this paper.

Throughout this section we work at the level of the individual parcel and derive the unit economics of the decision at this scale. All quantities are expressed on a per acre basis.

Dryness We denote by d_i the level of dryness in parcel i . The higher d , the more intensely dry the local climate is. We will drop the geographic subscript i to ease notations in this section.

Production Let the farming production on irrigated land be a fixed \bar{y} per acre independently of dryness conditions. It is the objective of the technology to insulate production against insufficient rain/moisture levels. We note returns to non-irrigated land $y(d)$ per acre, a decreasing function of the dryness level d . We assume that $y(0) = \bar{y}$. In words, the return from irrigated land is the same as the return from non-irrigated land if dryness is zero on average. This assumption is in line the rent of irrigated land with being close to equal to the rent of non-irrigated land in the counties with lowest dryness levels in the US as we showed in the previous section.

Adaptation Costs In order to produce output \bar{y} , farmers must pay two costs. First they need to pay for the infrastructure. We assume that there is a competitive rental market for water infrastructure and the equipment can be rented for a price \bar{p} per efficient unit of surface.

In addition, the infrastructure requires a local supply of water to deliver the optimal output. This functions as a completely local cost equal to $\frac{1}{1+\zeta}\bar{y}c_j(d)\frac{\iota^{1+\zeta}}{\zeta}$. Because surface and ground water resources are a local, idiosyncratic endowment, we assume that the cost is location-specific⁵. It scales with \bar{y} so that the amount of water needed scales with efficient units of surface rather than just surface. Combining fixed and variable cost, we obtain that extracting a quantity of water in j to irrigate a fraction ι of local surface is given by:

$$C_j(d_j, \iota) = \underbrace{\frac{1}{1+\zeta}c_j(d_j)\iota^{1+\zeta}\bar{y}}_{\text{Water Extraction}} + \underbrace{\bar{p}\iota\bar{y}}_{\text{Infrastructure}} \quad (7)$$

With $\zeta > 0$ so that the cost of bringing additional water onto a given parcel becomes marginally larger as the share of irrigated production increases. Intuitively, small amounts of water are relatively inexpensive to find and utilize, while large amounts of water require larger infrastructure that can pump water from further sources such as groundwater wells or less accessible surface waterbeds, increasing the marginal cost of providing water to a given location as volumes demanded increase. $c_j(d_j)$ represents the local variable cost of irrigation at full capacity ($\iota = 1$). This cost of extraction increases with the level of dryness d . Intuitively, prolonged drought reduces the supply of easily accessible water resources such as rain, rivers and lakes and limits the replenishment of shallow groundwater resources. We capture the effect of dryness on water scarcity through this channel of increasing cost of extraction.

Demand for adaptation Bringing production and water costs together, we obtain that the net output of irrigated parcel j given ι and \bar{p} is given by:

$$y_j(d_j, \iota) = y(d_j) + [\bar{y} - y(d_j)] \times \iota - \bar{p}\iota\bar{y} - \frac{\bar{y}c_j(d_j)}{1+\zeta}\iota^{1+\zeta} \quad (8)$$

We assume that the quantity ι is chosen to maximize (8). Proposition 1 summarizes the optimum.

⁵We abstract from negative externalities that could affect local water markets so that the cost of water on a given parcel only depends on decisions made on that parcel.

Proposition 1 (Local Adaptation Choice) *The optimal amount of irrigation investment demanded is given by:*

$$v_j^* = c_j(d_j)^{-1/\zeta} \left(\underbrace{\frac{\bar{y} - y(d_j)}{\bar{y}}}_{R(d_j)} - \bar{p} \right)^{1/\zeta} \quad (9)$$

if $R(d_j) \geq \bar{p}$ and 0 otherwise. Implied returns to farming on parcel j given by:

$$y_j(d, \bar{p}) = y(d_j) + \bar{y} \frac{\zeta}{1 + \zeta} (R(d_j) - \bar{p})^{\frac{1+\zeta}{\zeta}} c_j(d_j)^{-1/\zeta} \quad (10)$$

Comparative static: Adaptation investment is

- Locally increasing in the dryness level d if $\frac{R'(d)}{R(d) - \bar{p}} > \frac{c'(d)}{c(d)}$
- Locally decreasing otherwise

Proposition 1 shows that aside from the idiosyncratic cost component, investment in adaptation is determined by a fixed elasticity ζ over the adjusted return $R(d) - \bar{p}$. In particular, given the comparative static, it is possible to find a function $R(d)$ and a cost function $c(d)$ to rationalize the hump-shaped adoption pattern observed in Section 2.3. We discuss this point in more details below after establishing the model counterpart of our regression equation.

Link to the data We now express the quantities measured in the previous section within our theoretical framework. We will show that this simple model can accommodate and rationalize the stylized facts on irrigation adoption previously documented. We proceed by building the theoretical counterpart to the regressions run in the previous section.

County-level regressions We assume that the idiosyncratic cost component c_j is homogeneous at the level of the county i . This assumption finds support in the size of areas with homogeneous water stress level displayed in Figure 7. The idiosyncratic component c_j can be seen as a direct representation of an area's natural water resource endowment, which should be roughly constant at the scale of a county. We can then aggregate the above decision rule at the county level by summing over the surface of each parcel. We obtain that the surface irrigated in county i is equal to:

$$S_{it} = \int_{j \in i} S_j v_j^* dj = \int_{j \in i} S_j dj \times \left(\frac{R(d) - \bar{p}}{c_i(d)} \right)^{1/\xi} \quad (11)$$

The fixed effect specification from equation 5 directly estimates coefficient $a(d)$, the elasticity of log irrigated surface $\log(S_{it})$ with respect to d . Formally:

$$a(d) = \frac{\partial \log S_{it}}{\partial d} \quad (12)$$

We can solve for this elasticity in our model, which yields:

$$a(d) = \frac{1}{\xi} \left(\underbrace{\frac{R'(d)}{R(d) - \bar{p}}}_{\text{Increase in output protected}} - \underbrace{\frac{c'_i(d)}{c_i(d)}}_{\text{Water scarcity}} \right) \quad (13)$$

at different levels of dryness d .

Hump shaped irrigation adoption We find that the model can very easily accommodate the hump-shaped pattern of adoption measures in our regressions by calibrating the rate at which non irrigated land loses value relative to non irrigated land $R(d)$ and the cost function. Equation (13) shows that an increasing adoption profile $a(d) > 0$ is possible if the marginal benefit from installing a system grows faster with dryness than the cost associated with water scarcity. Conversely, the decreasing adoption pattern seen as high levels of dryness is consistent with water scarcity costs rising faster than the economic benefits from irrigation at these levels. This also corresponds to intuition: At mild levels of dryness, the increase in the cost of water extraction must be relatively small, yielding a relatively flat function $c(d)$ and small marginal cost $\frac{c'(d)}{c(d)}$. The cost of extraction becomes extremely high in very dry regions, where only expensive desalinization techniques or large infrastructure is required to add any elasticity to the local water supply. Finally notice that if the cost is directly related to our measure of water stress bwd , then we can directly interpret the second term in (13) as coefficient b_2 in 4 and the first term as coefficient b_1 . Hence our model rationalizes the hump-shaped adoption pattern observed in the data and our suggestive evidence on water scarcity driving this pattern.

Rents Rents are not a natural object in this model as the irrigation infrastructure is purchased at price \bar{p} per efficient unit of land by the farmer directly. We documented in the previous section that the agricultural land rental market is largely a

relationship market where landlords can exert significant market power. Hence we assume that the rent for non irrigated land P and for irrigated land P^{Irr} are determined by a Nash bargaining process between farmers and landlords. Landlords have bargaining power b . The outside options for both landlord and farmer give 0 payoff, hence the total surplus of production is divided according to:

$$\text{Max}_P P^b (y - P)^{1-b}$$

Where y is the total surplus from farming the parcel. The standard Nash bargaining solution to this problem states that players obtain their bargaining power as a share of the surplus. Formally $P = b \times y$, which can be applied to both irrigated (yielding P^{Irr}) and non irrigated (yielding $P(d)$) parcels. The surplus from non-irrigated land is simply $y(d)$. The surplus from irrigated land can be defined as the average profit of irrigated surface over parcel j :

$$y_j^{Irr}(d) = y(d) + \frac{1}{\iota} \int_{x=0}^{\iota} [\bar{y} - y(d) - \bar{y}\bar{p} - \bar{y}c_j(d) \frac{x^\zeta}{1+\zeta}] dx$$

Let $\bar{w} = \frac{1}{(1+\zeta)^2}$. Calculating the integral and injecting the value of ι given by Equation (9) yields:

$$y_j^{Irr}(d) = \bar{w}y(d) + (1 - \bar{w})\bar{y}(1 - \bar{p}) \quad (14)$$

Combining the two rents, we obtain that the irrigation rent premium is equal to:

$$R^{Irr}(d) = \frac{P^{Irr} - P(d)}{P^{Irr}} = \frac{y^{Irr}(d) - y(d)}{y^{Irr}(d)} = 1 - \frac{y(d)}{\bar{w}y(d) + (1 - \bar{w})\bar{y}(1 - \bar{p})} \quad (15)$$

According to Equation (15) we can assimilate the surplus from irrigating and the relative rent premium for irrigated land. The relative rent premium is exactly what we have used as our dependent variable in Section 2.2, and we can verify that our modeled quantity has the same properties as its empirical counterpart. In particular, it is a strictly decreasing function of $y(d)$. Assuming that $y(d)$ is monotonically decreasing in d , $R(d)$ is an increasing function of d as we found in our regression results presented in Table 2. As d nears 0, $y(d) \approx \bar{y}$ and the rent premium is approximately 0 as observed in Section 2.2. Conversely $y(d)$ goes to 0 as d becomes large. Hence the rent premium is monotonically increasing from 0 to 1 as d goes from 0 to its upper bound, which is what we observe empirically. To summarize, the model rationalizes the empirical agricultural rent and their variation with d if $y(d)$ is monotonically decreasing in d , validating one of our key modeling assumptions.

Hump shaped returns So far we have shown that it is possible to rationalize a strictly increasing irrigation premium and a hump shaped adoption pattern if the benefits to irrigation adoption (given by $R(d)$ or equivalently $\bar{y} - y(d)$) are increasing in d but increase less fast than the cost of water extraction $c(d)$. We will now show that within our model, these empirically motivated assumptions imply hump shaped returns to irrigation as an investment. Proposition 2 formalizes this finding.

Proposition 2 *Suppose that:*

- $c(d) \rightarrow +\infty$ as d increases
- $y(d)$ is monotonically decreasing in d
- Observed irrigated surfaces S_{it} defined in (11) increase then decrease as d increases or equivalently $a(d)$ defined in (13) decreases from positive to negative as d increases

Then the marginal return to irrigation investment is hump-shaped with respect to d , i.e. $\frac{\partial y}{\partial \iota}$ is increasing then decreasing as d increases.

Proof:

See Appendix B.2.

An illustration of the marginal return function $\frac{\partial y}{\partial \iota}$ is depicted on Figure 8 in the Appendix. It clearly shows the inverted U shape of the marginal product of investment. It also pictures the fact that a higher water demand given by a larger value of ι makes the marginal product of irrigation investment decrease even faster with d as it amplifies the impact of costs associated with rising water scarcity on returns.

Towards macroeconomic adaptation In this section we have built a partial equilibrium model of irrigation investment where the key assumptions about farming returns and water extraction costs are disciplined in a way that rationalizes the key findings from our empirical section. We then showed in Proposition 2 that a consequence of these assumptions is that returns to irrigation are hump shaped. This is a key property, which can be expressed in words as the fact that the technology loses efficiency as dryness becomes more extreme. In other words, irrigation presents a window of opportunity for climate change adaptation but will eventually be unable to help us if global warming is not contained.

3.2 Macroeconomic adaptation function

We now aggregate our microeconomic partial equilibrium model at the macroeconomic level. We will show that the resulting macroeconomic adaptation function is well-behaved and satisfies a similar property to the microeconomic returns, namely hump shaped marginal returns.

Global temperature anomaly Denote by ϵ the level of the global temperature anomaly with respect to pre-industrial conditions. This variable is a summary statistic for the intensity of global warming and maps to a specific stock of greenhouse gases in the atmosphere. We start by defining the mapping $d : \epsilon \rightarrow (d_i(\epsilon))_{i \in \mathcal{I}}$ which associates a level of the variable ϵ with a vector containing the dryness level of every location $i \in \mathcal{I}$ in the US.

Adaptation market clearing Given a price vector $p = (\bar{p}_i)_{i \in \mathcal{I}}$ denoting the price of irrigation infrastructure for each location i in the US, the aggregate amount of adaptation investment is given by:

$$\iota = \bar{y} \times \int_i S_i \iota_i(d_i, \bar{p}_i) di$$

We can now define the competitive equilibrium on the market for adaptation investment.

Definition 1 *The competitive equilibrium on the market for adaptation investment is the allocation of local investments $(\iota_i)_{i \in \mathcal{I}}$, prices $p = (\bar{p}_i)_{i \in \mathcal{I}}$ and aggregate investment level ι such that :*

1. *All local prices are equal : $\bar{p}_i = \bar{p}_j = \bar{p} \forall (i, j) \in \mathcal{I}$*
2. *Local demand for investment $\iota_i(d_i, \bar{p}_i)$ is defined by Proposition 1*
3. *The quantity of adaptation investment clears:*

$$\iota = \bar{y} \times \int_i S_i \iota_i(d_i, \bar{p}) di \tag{16}$$

The defined equilibrium respects the optimization problem of each individual parcel while setting an equal price for irrigation infrastructure everywhere. As a result it guarantees that the marginal product of irrigation infrastructure investment is the same everywhere: there no arbitrage between locations.

According to Proposition 1, all functions $\iota(d, \bar{p})$ are decreasing with respect to \bar{p} so that the right-hand side of Equation (16) is also monotonic in \bar{p} . Therefore choosing ι is exactly equivalent to choosing \bar{p} . In all that follows, we assume implicitly that the competitive equilibrium we just defined prevails. As a result all outcomes can be made a function of the choice variable ι , which denotes the aggregate supply of adaptation investment which becomes our main control variable. We note $\bar{p}(\iota)$ the unique price satisfying Equation (16) given ι .

Aggregate output The aggregate farming output is given by the sum of all local outputs:

$$\mathcal{Y}(\epsilon, \iota) = \int_i S_i y_i(d_i(\epsilon), \bar{p}(\iota)) di \quad (17)$$

The total stock of capital in this sector of the economy is the sum of all the farmland measured in terms of surface:

$$K = \int_i S_i di = \int_i K_i di \quad (18)$$

and aggregate production can then be expressed as an AK technology:

$$Y(\epsilon, \iota) = A(\epsilon, \iota) \times K \quad (19)$$

Where $A(\epsilon, \iota) = \int_i \frac{K_i}{K} y_i(d_i(\epsilon), \bar{p}(\iota)) di$

Macroeconomic adaptation We summarize the construction of the macroeconomic adaptation function $A(\epsilon, \iota)$ in Proposition 3 and establish its key properties.

Proposition 3 (Macroeconomic adaptation function) *We define the aggregate adaptation function as:*

$$A(\epsilon, \iota) = \int_i \frac{K_i}{K} y_i(\epsilon, \iota) di \quad (20)$$

Where:

- $K_i = S_i$ is the local stock of capital in county i
- $K = \int_i K_i di$ is the aggregate stock of capital

- *Local output is given by:*

$$y_j(\epsilon, \iota) = y(d_j(\epsilon)) + \bar{y} \frac{\zeta}{1 + \zeta} \left(\text{Max} \left(\frac{\bar{y} - y(d_j(\epsilon))}{\bar{y}} - \bar{p}(\iota), 0 \right) \right)^{\frac{1+\zeta}{\zeta}} c_j(d_j(\epsilon))^{-1/\zeta} \quad (21)$$

- *And $\bar{p}(\iota)$ is the unique solution to:*

$$\iota = \bar{y} \times \int_j S_j c_j(d_j(\epsilon))^{-1/\zeta} \left(\text{Max} \left(\frac{\bar{y} - y(d_j(\epsilon))}{\bar{y}} - \bar{p}, 0 \right) \right)^{1/\zeta} dj \quad (22)$$

So that aggregate output can be written:

$$Y(\epsilon, \iota) = A(\epsilon, \iota) \times K \quad (23)$$

The macroeconomic adaptation function $A(\epsilon, \iota)$ has the following properties:

- Regularity: *It is continuous and derivable everywhere*
- Monotonicity: *It is decreasing in ϵ if all local $d_i(\epsilon)$ are increasing in ϵ . It is decreasing in each individual $d_i(\epsilon)$. It is increasing in ι .*
- Weakly decreasing marginal returns: *It is weakly concave (i.e. strictly concave or linear) in ι for all ϵ as a sum of increasing and concave/linear functions of ι .*
- Asymptotically hump shaped: *$\frac{\partial A}{\partial \iota}$ is increasing in ϵ for $\epsilon \rightarrow 0$ and decreasing for ϵ large enough*

Proof:

The three first claims are trivially verified as the function is a sum of individual functions displaying the same regularity properties. The last one relies on an asymptotic argument. The asymptotic hump-shaped profile is a direct consequence of summing individual functions $y(\iota, \epsilon)$ which all have derivatives $\frac{\partial y}{\partial \iota}$ that are hump-shaped with respect to ϵ . Taking the limit of this sum as ϵ goes to 0 or grows very large, we obtain a sum of functions that are all increasing (resp. decreasing) with respect to ϵ , proving the claim.

Micro-foundation Proposition 3 is the basis for our micro-foundation of realistic adaptation functions in integrated assessment models. Of particular interest will be the properties of decreasing marginal returns guaranteeing well-behaved macro-level optimization and the humped shape of the returns to adaptation. The latter, although asymptotic in this proposition, will be central to the theoretical contribution of this paper developed in the next section.

Towards integrated assessment models The main obstacle to using our micro-founded properties in a broader macro-level adaptation investment problem is their generality to the broader set of adaptation technologies available to the social planner. Indeed adaptation is not limited to irrigation nor even to agriculture. Hence we conclude this section with a discussion on the generality of the hump-shaped protection profile property. We will then build on our findings to explore the impact of this property for macro-level adaptation in a stylized climate macro-finance model embedding the main features of modern integrated assessment models.

3.3 Generalization

As we generalize our model to the broader context of adaptation to climate change, the first step is to introduce a more general definition of adaptation investment. We henceforth define "adaptation" as a technology or process that has no intrinsic productive value (it is not a final good nor participates in the process of production of one) but can reduce the damages caused by climate change. Irrigation typically falls into this category. We finish our micro-foundation exercise by discussing other major climate adaptations and argue that they all exhibit the same hump-shaped returns property we uncovered for irrigation.

Example 1. Adapting to heatwaves The first example of adaptation to rising temperatures that comes to mind is the use of cooling technologies (e.g. air conditioning) to restore productivity levels and limit harmful health consequences. As temperatures increase, the cost of maintaining productivity and welfare to its "no warming" counterfactual is largely convex. At small temperature increases, simple indoor air conditioning systems can be sufficient to maintain welfare levels roughly unaffected at a very small cost. As temperatures become more extreme, outside activities become impossible without heavy protection and, for the most extreme heatwaves, can induce life-threatening consequences. The costs of maintaining output equal to a no warming counterfactual under a climate that makes such extreme events a frequent occurrence would raise exponentially. Hence the protection profile of technological adaptations to heatwave also display a hump-shaped protection profile.

Example 2. Adapting the electric grid to extreme weather The electric grid is a central concern with the rise in intensity of winter storms and wildfires. Indeed, the transmission and distribution infrastructure is largely exposed to these damaging events causing billions of damages in repairs, loss of power and economic activity.

As climate change is responsible for an increase in the intensity and frequency of these events, several adaptation strategies exist. It is relatively inexpensive to adapt the grid to "mild" winds and cold by "hardening" the lines and ensuring that no nearby tree or structure might fall and damage infrastructure. For extreme storms or heat, only the complete undergrounding (an extremely costly measure) of electric infrastructure can possibly mitigate the damages. Recent occurrences such as storm Elliott in the U.S. North-East have shown that generators themselves were at risk of failure, making adaptation almost impossible in the most extreme cases⁶. Therefore the protection profile in this case is also hump-shaped.

Example 3. Adapting to storm surges and hurricanes Storms and hurricanes are amongst of the most damaging climatic events that can occur, and recent evidence suggest that climate change is increasing their intensity. This has led to a series of adaptations such as building seawalls and drainage systems to limit the damages of the resulting floods. These systems also display a hump-shaped protection profile as increasingly intense shocks require always higher walls and always more resistant buildings and powerful drainage systems at largely convex (if even achievable) costs.

Window of opportunity Given these examples and the concrete case of irrigation studied in the previous section, we posit that the assumption of hump-shaped returns to adaptation technology is a reasonable one from a macro-economic perspective. In words, we argue that adaptation technologies should be modeled as a "window of opportunity" investment whose returns peak before decreasing as climate change becomes more intense. We now turn to a simple stylized model that incorporates this technological feature to explore its consequences. We will focus in particular on how it interacts with ambiguity about future climate.

4 Stylized macroeconomic model

4.1 Setup

In order to build intuition, we propose a simple model that features two periods $t = 0, 1$.

⁶<https://www.ferc.gov/media/analysis-pjms-winter-storm-elliott-report-2023>

Resource constraint There is an initial endowment y_0 at period 0 that can be used for consumption in that same period c_0 , building productive capital K or investing into an adaptation technology ι . This yields the resource constraint:

$$y_0 = c_0 + K + \iota \quad (\text{Resource Constraint})$$

Climate change There is a state of the world which denoted by ϵ and represents the global temperature anomaly, i.e. the intensity global warming directly mapped to the stock of greenhouse gases in the atmosphere. It is a random variable and we describe its influence below.

Production Production is given by the following AK technology:

$$y = A(\epsilon, \iota)K \quad (24)$$

Where $A(\epsilon, K)$ is a productivity term that depends on the macroeconomic state ϵ and the amount of adaptation spending ι . The difference between this setup and the previous section is that two opportunities for investment co-exist: agents can either invest into adaptation ι or grow the stock of capital K which becomes an endogenous object.

Adaptation function We lay out the main properties of the adaptation function. First we impose that output is decreasing as climate change intensifies:

$$\frac{\partial A}{\partial \epsilon} < 0 \quad (\text{A1})$$

Investment into the adaptation technology ι weakly increases output and has decreasing returns

$$\frac{\partial A(\epsilon, \iota)}{\partial \iota} \geq 0 \ \& \ \frac{\partial^2 A(\epsilon, \iota)}{\partial \iota^2} < 0 \quad (\text{A2})$$

Adaptation spending can only protect output from damages linked to climate change and therefore production is bounded above by its "no warming" counterfactual:

$$A(\epsilon, \iota) \leq A(0, 0) \ \forall (\epsilon, \iota) \quad (\text{A3})$$

Protection profile We now incorporate the hump shape of the protection profile. Formally, we assume that there exists $\bar{\epsilon}$ such that the marginal benefit of an extra unit of adaptation spending is increasing below that level and decreasing beyond:

$$\frac{\partial^2 A}{\partial \iota \partial \epsilon} \begin{cases} > 0 \text{ if } \epsilon < \bar{\epsilon} \\ < 0 \text{ if } \epsilon > \bar{\epsilon} \end{cases} \quad (25)$$

Preferences and optimization The social planner maximizes expected utility over the two periods subject to the recourse constraint. The period utility function u is canonical, i.e. strictly increasing and concave in consumption. The maximization problem of the planner is the following:

$$\text{Max}_{\iota, K} u(y_0 - \iota - K) + \beta \mathbb{E}(u(A(\epsilon, \iota)K))$$

Proposition 4 (Stylized model solution)

In equilibrium we have two cases:

1. *Either $\iota > 0$ and the solution for (ι^*, K^*) is given by the following system of equations:*

$$\beta \mathbb{E}_\epsilon \left(\frac{u'(A(\epsilon, \iota^*)K^*)}{u'(y_0 - K^* - \iota^*)} A(\epsilon, \iota^*) \right) = 1 \quad (26)$$

$$\beta K \mathbb{E}_\epsilon \left(\frac{u'(A(\epsilon, \iota^*)K^*)}{u'(y_0 - K^* - \iota^*)} \frac{\partial A}{\partial \iota}(\epsilon, \iota^*) \right) = 1 \quad (27)$$

2. *Or $\iota = 0$ and capital investment is given by:*

$$\beta \mathbb{E}_\epsilon (u'(A(\epsilon, 0)K)) = u'(y_0 - K^* - \iota^*) \quad (28)$$

In order to interpret the previous proposition, let us define the stochastic discount factor (SDF):

$$m(\epsilon) = \beta \frac{u'(A(\epsilon, \iota^*)K^*)}{u'(y_0 - K^* - \iota^*)}$$

As utility is concave, m is increasing in ϵ : marginal consumption is valued more in states with high risk realization and lower overall consumption. We also define the risk-free rate $\frac{1}{1+r} = \mathbb{E}(m)$. While Equation (26) simply depicts no arbitrage between current consumption and returns to productive capital and is classic, the second is core to the argument of this paper.

Protection profile of adaptations We can re-write equation (27):

$$K \mathbb{E}_\epsilon \left(m(\epsilon) \frac{\partial A(\epsilon, \iota^*)}{\partial \iota^*} \right) = 1 \quad (29)$$

Notice that the marginal benefit of adaptation materializes through a partial derivative within the parenthesis: it modifies the risk profile associated with productive capital for each realization of ϵ . We can re-write the above expression:

$$\underbrace{\frac{K}{1+r} \mathbb{E}_\epsilon \frac{\partial A(\epsilon, \iota^*)}{\partial \iota^*}}_{\text{Average utility protected}} + \underbrace{K \text{Cov}_\epsilon \left(m(\epsilon), \frac{\partial A(\epsilon, \iota^*)}{\partial \iota^*} \right)}_{\text{Insurance against worst scenarios}} = 1 \quad (30)$$

Where $1/(1+r)$ is defined as the expected stochastic discount factor as is standard in the macro-finance literature. The marginal benefit of adaptation can be broken down into two terms. The first one is straightforward: it is the expected discounted damage avoided and integrates the protection profile $\frac{\partial A(\epsilon, \iota)}{\partial \iota}$ over the full spectrum of potential realizations of future climate ϵ .

Insurance against ambiguity The second term is most interesting as it depicts a macroeconomic insurance premium. Indeed, at the second order in ϵ around $\tilde{\epsilon}$, the second term can be written:

$$\text{Cov}_\epsilon \left(m(\epsilon), \frac{\partial A(\epsilon, \iota^*)}{\partial \iota^*} \right) \approx_{\tilde{\epsilon}} m'(\tilde{\epsilon}) \frac{\partial A(\tilde{\epsilon}, \iota^*)}{\partial \iota \partial \epsilon} \sigma_\epsilon^2 \quad (31)$$

This approximation lets three terms appear. Firstly $m'(\tilde{\epsilon})$ is the variation in stochastic discount factor due to a change in ϵ . It captures the premium that households are willing to pay to increase consumption at different levels of ϵ . As production and consumption c_1 decrease with the intensity of climate change ϵ , we have $m'(\epsilon) > 0$.

The sign of the above expression is the same as the sign of the second term: the cross derivative of the marginal product of capital with respect to adaptation and ϵ . This term captures the risk premium attached to adaptation investment. If it is positive, adaptation investment provides insurance against the risk of extreme climate change scenarios. If it is negative, adaptation investment's payoff is made worse in worst states of the world, imposing a premium to its marginal return. Finally, the last term σ_ϵ^2 captures the degree of uncertainty about future climate. The larger uncertainty, the larger the premium or discount to the returns of the technology for its capacity to hedge against the worst climate scenarios.

Link with the protection profile Notice that due to our assumption of hump-shaped protection profile, this term is negative if $\tilde{\epsilon} > \bar{\epsilon}$. The fact that adaptations lose in efficiency as climate change becomes more severe has two consequences. The first is to decrease the average expected output loss from climate change, represented by the first term in Equation (30). The second is to make adaptation very sensitive to the degree of uncertainty through the second term (the risk premium), which is

a novel finding. This sheds a different light on the stakes of the political economy of our pledges to reduce emissions. The expected scenario matters but the degree of uncertainty surrounding our commitment to these pledges also has real consequences by hurting the viability of current adaptation technologies.

Irreversibility of investment We emphasize that the main feature of the two period model producing the uncertainty-related result is the irreversibility of adaptation investment. If adaptation was perfectly reversible, the best strategy could be adopted as uncertainty resolves without a need for anticipation. In this case, one could wait to obtain a very good signal about the realization of ϵ before making the adaptation decision. While strict irreversibility exists in our simplistic 2 periods model, adjustment costs that limit the speed at which adaptation can be adjusted are sufficient to obtain the above effect. A long-standing literature studies the consequences of capital investment irreversibility in the context of business cycle uncertainty (Pyndick 1982 (22), Bertola & Caballero 1994 (5), Kogan 2001 (18)). This literature emphasizes that irreversibility generates inertia: investment is hindered by large uncertainty because of the possibility to get capital levels wrong and not being able to revert the investment. We demonstrated through Equation (30) that this inertia phenomenon is also central for adaptation to climate change and that it is linked to the protection profile. Indeed, as the local approximation in Equation (31) demonstrates, it is the variation of the marginal product of adaptation with ϵ that determines the sign of the risk premium.

4.2 Illustration

We now turn to an illustration of the dynamics of the stylized model presented in Section 3.3. We will show that the adaptation investment dynamics mirror the hump-shaped adoption pattern discussed in section 2.2, discuss a stylized version of the cost of carbon and emphasize the role of uncertainty in shaping the optimal adaptation policy.

Adaptation function We use the following functional form for the macroeconomic adaptation function:

$$A(\epsilon, \iota) = 1 - \alpha\epsilon \left(1 - \min\left(\frac{\iota^\kappa}{\theta} e^{-h\epsilon}, 1\right) \right) \quad (32)$$

We verify in Proposition 6 in the appendix that the function $A(\epsilon, \iota)$ defined in (32) satisfies the properties (A1), (A2) and (A3). We also assume to simplify exposition that ϵ lives on a domain where output is always positive (α sufficiently small). Two illustrations of the function are provided for different parameter values. First Figure 2 shows A as a function of ϵ for two different values of h . We discuss the significance of this parameter below. Second Figure 9 in the appendix shows the influence of parameters κ and θ with a different perspective on ι and ϵ .

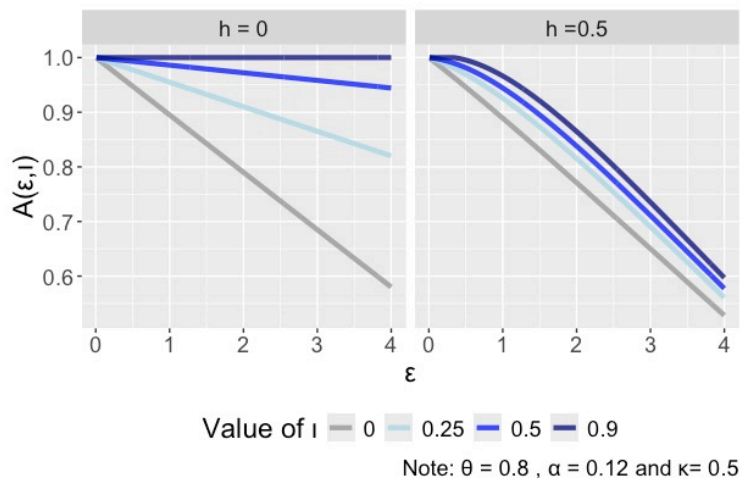


Figure 2: $A(\epsilon, \iota)$ for different values of ι and ϵ

Absent any adaptation spending, output is a simple linear function of ϵ :

$$A(\epsilon, 0) = 1 - \alpha\epsilon$$

Positive adaptation spending diminishes the influence of ϵ . It lowers the slope from α , which would have represented the elasticity of output with respect to temperature absent any adaptation. To build intuition about the influence of ι , we can express:

$$\phi(\iota, \epsilon) = \frac{\iota^\kappa}{\theta} e^{-h\epsilon} \quad (33)$$

ϕ represents the fraction of total damages that is prevented by the current level of adaptation investment given a realization ϵ of climate change. If $h = 0$, notice that this fraction is constant: adaptation has an increasing payoff proportional to the damages. This is the first case depicted in Figure 2. Conversely as $h > 0$ increases and returns become hump-shaped, the fraction of damages prevented by

adaptation is decreasing faster with ϵ . Hence the parameter h controls the pace at which technological adaptation will lose efficiency as global temperature increases. An illustration is given in the second panel of Figure 2. Finally, θ and κ are two parameters that govern the efficiency of the adaptation technology. In particular, κ controls the degree of concavity and θ is a scale parameter to set the initial slope. Their influence is shown in Figure 9 in the appendix.

Preferences We assume a CRRA utility function parametrized by risk aversion parameter γ :

$$u(c) = \frac{c^{1-\gamma}}{1-\gamma} \quad (34)$$

Solution of the model The solution of the model presented in Proposition 4 can be expressed as a system of non linear equations with special cases. We derive it in the appendix and present the equations of interest in Proposition 5 below. Note that we do not have a corner case with no adaptation because we parametrized the adaptation function to have infinite marginal return at 0, a convenient but not necessary addition from the setup of the previous proposition to simplify the dynamics.

Proposition 5 (Illustrative Solution)

Let $\psi(\epsilon)$ be the pdf of the distribution of ϵ . Let $\bar{\epsilon}$ be the maximum of the support of the distribution of ϵ .

Given the functional forms (34) and (32) for utility and the adaptation function, the equilibrium levels of consumption and investment are characterized by a system with two distinct cases.

Either (c_0^*, ι^*, K^*) are jointly determined by the system:

$$c_0^* = y_0 - K^* - \iota^* \quad (35)$$

$$\frac{K^*}{y_0 - \iota^* - K^*} = \beta^{1/\gamma} \left(\int A(\epsilon, \iota^*)^{1-\gamma} \psi(\epsilon) d\epsilon \right)^{1/\gamma} \quad (36)$$

$$\left(\int A(\epsilon, \iota^*)^{1-\gamma} \psi(\epsilon) d\epsilon \right) = K^* \mathbb{E} \left(A(\epsilon, \iota^*)^{-\gamma} \frac{\partial A}{\partial \iota} \right) \quad (37)$$

If ι^* given by this previous system is such that $\iota^* > (\theta e^{h\bar{\epsilon}})^{1/\kappa}$, then the equilibrium is instead defined by (35), adaptation investment given by:

$$\iota^* = (\theta e^{h\bar{\epsilon}})^{1/\kappa} \quad (38)$$

and equation (36) which simplifies to:

$$K^* = \frac{\beta^{1/\gamma}}{1 - \beta^{1/\gamma}}(y_0 - \iota^*) \quad (39)$$

Deterministic Solution We start by assuming that ϵ is deterministic. We solve the system presented in Proposition 5 for an interval of values of ϵ and present the results of the simulation in Figure 3. Note that when we assume that ϵ is deterministic, the objective can be either strictly concave or have a concave and a linear part. This happens if we set the resources of the economy y_0 so that it is optimal to "max out" on adaptation, which corresponds to case 2 of Proposition 5. We show the adaptation choice ι^* on the top panel of Figure 3. The pattern is hump-shaped as we observed in the case of irrigation in the first section of this study. It is particularly interesting to note that this implies completely opposite policies in optimistic and pessimistic climate scenarios. A lot of adaptation takes place in the former while none happens in the latter. Anticipating on our next argument, this has consequences for the decision to adapt under uncertainty as it implies that the more hump-shaped the adaptation function is, the narrower the window of opportunity is and therefore the costlier uncertainty will be for the technology. The third panel shows a normalized social cost of carbon, assuming that the global temperature is a linear function of the total amount of carbon in the atmosphere as is standard in the literature. We can see that the social cost of carbon is lower at intermediate scenarios due to the positive impact of adaptation. Unfortunately this benefit dissipates as climate change becomes more intense. It is the visual illustration of the notion of "window of opportunity". If adaptation technologies display the same profile as today's available technologies, we cannot count on them to alleviate the damages from climate change in extreme scenarios. Re-phrasing this statement in a more positive light, the benefits to adaptation can be substantial if climate change is contained. This implies even larger incentives to aggressively commit to ambitious emissions reduction targets than current integrated assessment models are currently quantifying as they do not implement this technological adaptation margin.

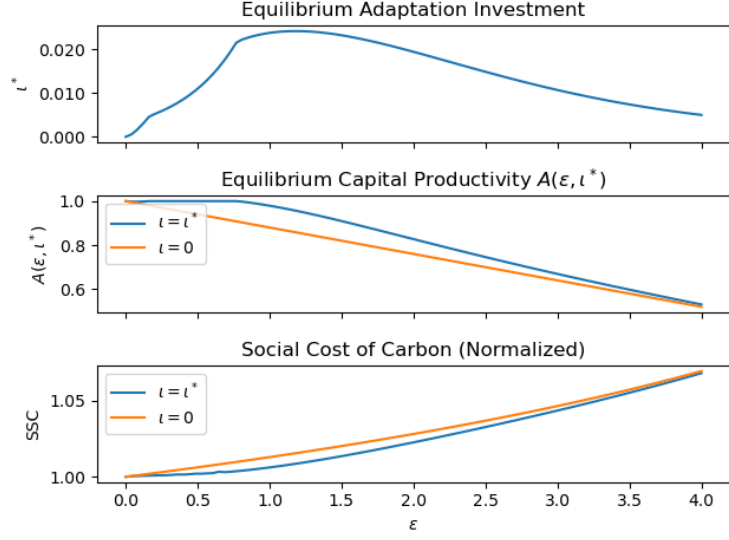


Figure 3: Adaptation investment and normalized social cost of carbon in the deterministic case

Effect of uncertainty Our final exercise is to show the link between uncertainty and h , our parameter controlling how fast adaptation efficiency is declining for high ϵ . h also controls the degree to which returns are hump-shaped as we showed on Figure 2. In order to simulate the model, we set the distribution of ϵ to a standard normal $\mathcal{N}(\mu, \sigma)$. Maintaining the mean μ constant will maintain the "adaptation-free" expected damages constant. Our exercise consists in observing the consequences of increasing σ for different levels of h to discuss the impact of uncertainty and its link with h . It would have been ideal to keep expected damages fixed while varying uncertainty and h to simulate a pure mean-preserving spread, but this is not possible as endogenous adaptation implies that a mean-preserving spread for one value of ι is not a mean-preserving spread for another value of ι . Hence keep in mind in our interpretation of the comparative statics that changing h also changes expected damages positively, which incentivizes more adaptation investment independently of uncertainty. Results of our simulations for three values of h are shown in Figure 4.

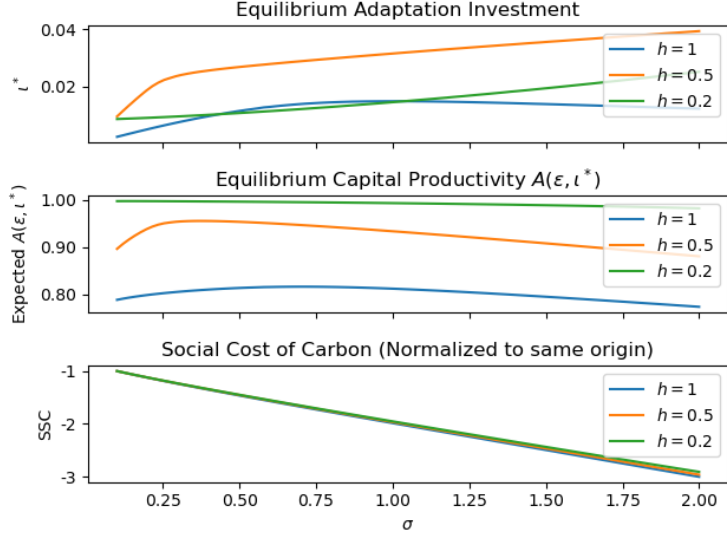


Figure 4: Comparative static with respect to σ for different values of h

The shape of the normalized social cost of carbon and productivity is not surprising: as uncertainty grows, large value of ϵ are more likely and risk aversion implies that these very bad outcomes are punished heavily in terms of welfare. Productivity looks hump-shaped as the planner weighs investing into the productivity term through adaptation and simply adding more capital. The most interesting outcome is the first panel of Figure 4 as it shows the effect of inertia. At very low h , we can see that adaptation investment is almost linearly increasing with uncertainty. Indeed for a low h , adaptation almost doesn't lose efficiency as ϵ grows. As a result, its profile looks almost flat. It is only slightly increasing because σ has an impact on expected damages, incentivizing more adaptation. The same argument explains why $h = 0.5$ features even higher adaptation levels, this time with a slight curvature. Finally, the case $h = 1$ shows adaptation levels that are strictly decreasing beyond a certain level of uncertainty. Looking back at the first panel of Figure 3 is key to understand this pattern: adaptation is only strongly used around $\epsilon = 1.5$ and is otherwise almost not invested into. As uncertainty grows, the chances of falling within the window of opportunity where adaptation is effective diminish, while the chances to see a scenario where it is useless are growing. This is why the hump shape, or "window of opportunity" pattern displayed by adaptation technologies has important consequences for the welfare cost of uncertainty. To put it simply: the narrower the window of opportunity, the higher the chances of getting adaptation levels wrong. As a result high uncertainty lowers the incentives to invest into adaptation and leads

to inertia.

Inertia This inertia phenomenon is absent from Hong & al. (16) because they allow adaptation levels to adjust instantaneously as a control, and to the best of our knowledge from the rest of the related climate finance literature. It is the contribution of this paper to show that this phenomenon exists in the case of adaptation to climate change and that it is tightly linked to the hump-shaped return profile of adaptation technologies. We also demonstrated in our empirical section that irrigation, a cornerstone of agricultural adaptation to climate change, exhibits this pattern of returns and discussed its prevalence among currently available technologies.

In a realistic setup where adaptation investments are massive and require years of commitment, such as building a sea wall, investing in desalination plants and technologies or burying thousands of miles of electric lines, we believe that the issue of inertia will be a critical one. This constitutes an additional incentive for policymakers to reduce uncertainty about future climate through better commitment devices (institutional arrangements, multilateral organizations...) and research efforts to make the underlying science more accurate and improve predictions.

5 Conclusion

In conclusion, this paper makes several contributions to the literature studying adaptation to climate change and supports the effort to build realistic integrated assessment models.

First we studied the concrete case of irrigation in US agriculture. We focused on this sector because it is most at risk from increased dryness and emerging water scarcity brought by climate change. In the US, we measured that irrigation - the main adaptation technique for agriculture at scale - has increased where dryness has mildly progressed but decreased where dryness has become the most intense. We then showed that willingness to pay for irrigation systems as measured by rent premia is strictly increasing in dryness, implying that the technology would be adopted if available. We found strong evidence that water scarcity - itself caused by climate change - is the underlying cause of the decrease in irrigated surfaces.

We then showed that a model of irrigation investment with convex water extraction costs (scarcity effect) rationalizes these findings. The model implies that the technology has humped-shaped returns: it is only effective within a certain window of opportunity and can't mitigate damages at extreme levels of dryness. Building on this framework, we showed that micro-level adaptation decisions can be aggregated

into a well behaved macroeconomic adaptation function that inherits this "window of opportunity" pattern. While this process was only applied to our irrigation case, we hope that our example can inspire similar calibration exercises for other sectors of the economy and other types of disasters such as coastal flooding, wildfires, heat-waves or hurricanes. There is a large avenue for future research in the quantification of suitable adaptation functions for most sectors to calibrate integrated assessment models that are still lacking this adaptation margin completely.

Finally we generalized our discussion to adaptation beyond the case of irrigation. In a stylized macroeconomic model where the humped-shaped property of adaptation returns is maintained, we showed that adaptation investment is high for mild climate change scenarios and decreases as climate change becomes more intense consistently with the "window of opportunity" pattern. Welfare and the social cost of carbon are accordingly higher (respectively. lower) than under the no adaptation counterfactual at contained global warming values but similar in extreme warming scenarios. Thus we qualitatively illustrate the expected effect of including adaptation with humped-shaped returns to integrated assessment models.

Adding uncertainty, our model delivers insights standard to finance theory but new to the discussion on climate adaptation. Uncertainty about future climate induces uncertainty about the payoff of adaptation technologies and about future consumption. Unfortunately, if the humped shape property of returns holds in the aggregate, adaptation technologies are not a good hedge against the worst states of the world. In economic terms, they lose value when marginal utility is highest. As a result, they bear a risk premium: at equal expected payoff, uncertainty reduces adaptation investment. This finding bears important consequences for the political economy surrounding climate change. This implies potentially important real effects for functioning multilateral institutions and other effective commitment devices that can reduce uncertainty about the future of climate change.

References

- [1] Jawad M Addoum, David T Ng, Ariel Ortiz-Bobea, and Harrison Hong. Temperature shocks and establishment sales. *The Review of Financial Studies*, 33(3):1331–1366, 2020.
- [2] Jenny C Aker and Kelsey Jack. Harvesting the rain: The adoption of environmental technologies in the sahel. Working Paper 29518, National Bureau of Economic Research, November 2021.
- [3] Christoph Albert, Paula Bustos, and Jacopo Ponticelli. The effects of climate change on labor and capital reallocation. Working Paper 28995, National Bureau of Economic Research, July 2021.
- [4] Matteo Benetton, Simone Emiliozzi, Elisa Guglielminetti, Michele Loberto, and Alessandro Mistretta. *Does Climate Change Adaptation Matter? Evidence from the City on the Water*. SSRN, 2023.
- [5] Giuseppe Bertola and Ricardo Caballero. Irreversibility and aggregate investment. *The Review of Economic Studies*, 61(2):223–246, 1994.
- [6] Adrien Bilal and Esteban Rossi-Hansberg. Anticipating climate change across the united states. Working Paper 31323, National Bureau of Economic Research, June 2023.
- [7] Leah Platt Boustan, Matthew E. Kahn, Paul W. Rhode, and Maria Lucia Yanguas. The effect of natural disasters on economic activity in us counties: A century of data. *Journal of Urban Economics*, 118:103257, 2020.
- [8] Bruno Conte, Klaus Desmet, Dávid Krisztián Nagy, and Esteban Rossi-Hansberg. Local sectoral specialization in a warming world. Working Paper 28163, National Bureau of Economic Research, December 2020.
- [9] José-Luis Cruz and Esteban Rossi-Hansberg. The economic geography of global warming. Working Paper 28466, National Bureau of Economic Research, February 2021.
- [10] Allison Borchers Daniel Bigelow and Todd Hubbs. Us farmland ownership, tenure and transfer. *Economic Information Bulletin Number 161*, (161), 2016.

- [11] Klaus Desmet, Robert E. Kopp, Scott A. Kulp, Dávid Krisztián Nagy, Michael Oppenheimer, Esteban Rossi-Hansberg, and Benjamin H. Strauss. Evaluating the economic cost of coastal flooding. *American Economic Journal: Macroeconomics*, 13(2):444–86, April 2021.
- [12] Oliver Giesecke, Dhruv Singal, and Jessica Goldenring. Economic impact of water scarcity. Working paper, National Bureau of Economic Research, February 2022.
- [13] Graeme Guthrie. Real options analysis of climate-change adaptation: investment flexibility and extreme weather events. *Climatic Change*, 156(1):231–253, 2019.
- [14] I. Haqiqi, D. S. Grogan, T. W. Hertel, and W. Schlenker. Quantifying the impacts of compound extremes on agriculture. *Hydrology and Earth System Sciences*, 25(2):551–564, 2021.
- [15] Harrison Hong, Frank Weikai Li, and Jiangmin Xu. Climate risks and market efficiency. *Journal of Econometrics*, 208(1):265–281, 2019. Special Issue on Financial Engineering and Risk Management.
- [16] Harrison Hong, Neng Wang, and Jinqiang Yang. Mitigating disaster risks in the age of climate change. Working Paper 27066, National Bureau of Economic Research, April 2020.
- [17] Solomon M Hsiang and Amir S Jina. The causal effect of environmental catastrophe on long-run economic growth: Evidence from 6,700 cyclones. Working Paper 20352, National Bureau of Economic Research, July 2014.
- [18] Leonid Kogan. An equilibrium model of irreversible investment. *Journal of Financial Economics*, 62(2):201–245, 2001.
- [19] M.F.P. Bierkens S. Lakshman T. Luo L. Saccoccia E. H. Sutanudjaja Kuzma, S. and R. Van Beek. Aqueduct 4.0: Updated decision-relevant global water risk indicators. Technical note, World Resources Institute, 2023.
- [20] William D. Nordhaus. The 'DICE' Model: Background and Structure of a Dynamic Integrated Climate-Economy Model of the Economics of Global Warming. Cowles Foundation Discussion Papers 1009, Cowles Foundation for Research in Economics, Yale University, February 1992.

- [21] U.S. Bureau of Economic Analysis. "gross domestic product by county and metropolitan area" and "employment by county, metro and other areas". Technical report. URL: <https://www.bea.gov/data/economic-accounts/regional>
- [22] Robert Pindyck. Adjustment costs, uncertainty, and the behavior of the firm. *American Economic Review*, 72(3):415–27, 1982.
- [23] Ivan Rudik. Optimal climate policy when damages are unknown. *American Economic Journal: Economic Policy*, 12(2):340–73, May 2020.
- [24] Ivan Rudik, Gary Lyn, Weiliang Tan, and Ariel Ortiz-Bobea. The Economic Effects of Climate Change in Dynamic Spatial Equilibrium. Technical report, 2022.
- [25] Charles A. Taylor. *Irrigation and Climate Change: Long-run Adaptation and its Externalities*. NBER, 2023.

Appendices

A Empirical Appendix

A.1 Figures

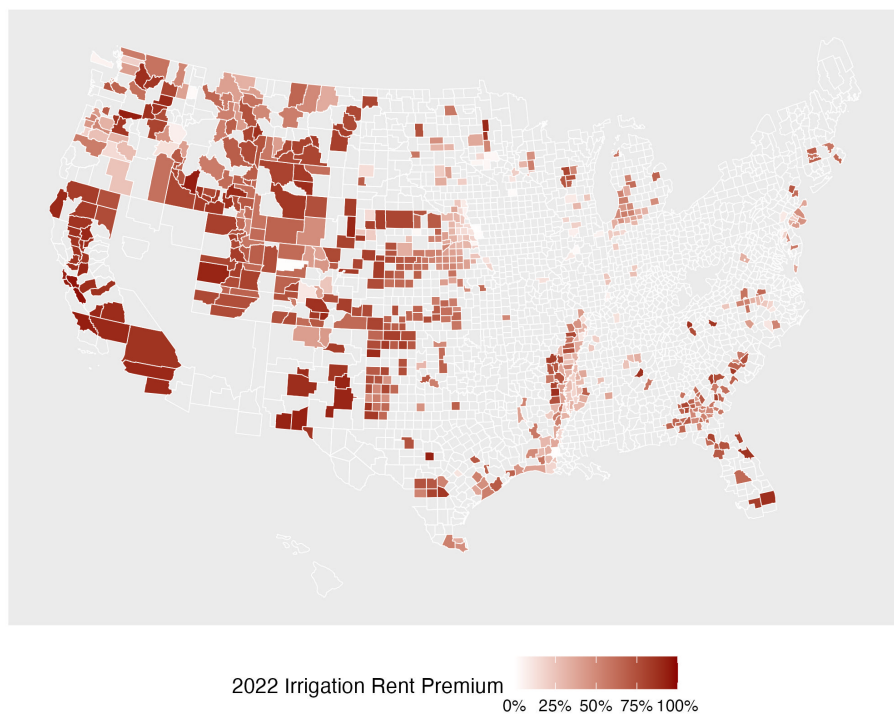


Figure 5: 2022 irrigation rent premium by county

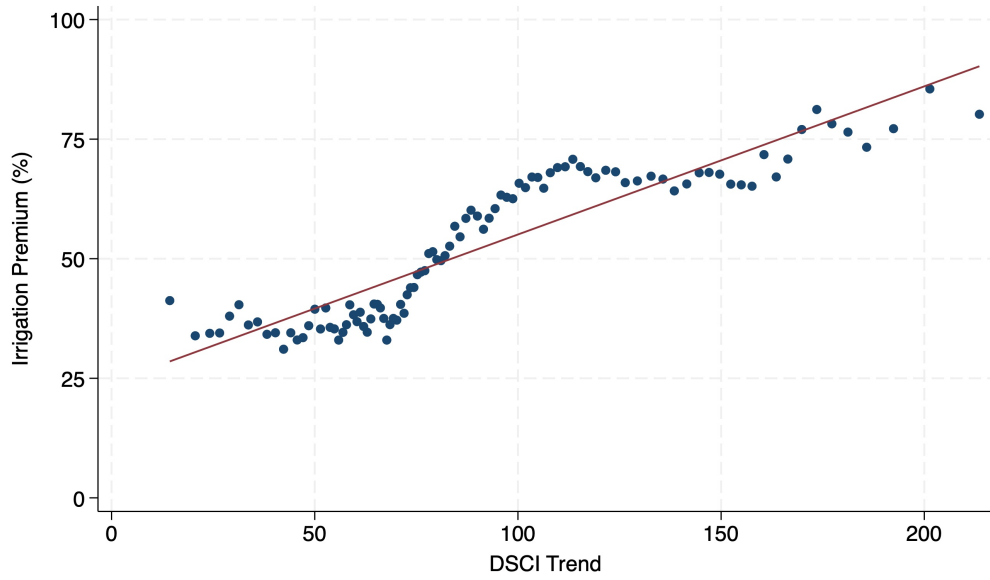


Figure 6: Quintile-binned scatterplot and linear fit of Irrigation Premium and 5year averaged DSCI

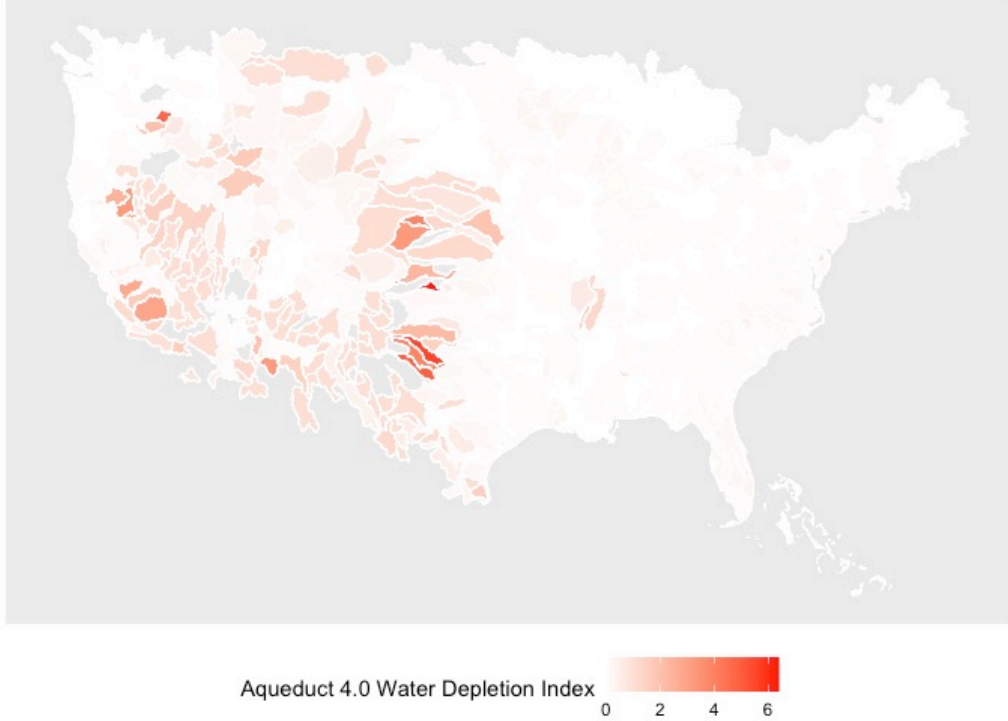


Figure 7: Aqueduct 4.0 base water depletion index (large values mean higher depletion rates)

A.2 Estimation Results

Quadratic Irrigation Premium Regression The quadratic regression equation is :

$$P_{it}^{Irrig} = r_0 \bar{d}_{i,t \rightarrow t-5} + r_1 \bar{d}_{i,t \rightarrow t-5}^2 + \alpha_i + \delta_t + \epsilon_{i,t} \quad (40)$$

Note that the average drought trend has been standardized to mean 0 and unit standard deviation.

<i>Dependent variable:</i>	
Irrigation Premium	
r_0	-0.022** (0.011)
r_1	0.014*** (0.003)
Observations	7671
Effects	County & Year
<i>Note:</i>	*p<0.1; **p<0.05; ***p<0.01

Table 5: Irrigation premium quadratic regression results

Quadratic Irrigation Surface Regression The quadratic regression equation is :

$$\log(S_{it}^{Irrig}) = a_0\bar{d}_{i,t \rightarrow t-5} + a_1\bar{d}_{i,t \rightarrow t-5}^2 + \alpha_i + \delta_t + \epsilon_{i,t} \quad (41)$$

Note that the average drought trend has been standardized to mean 0 and unit standard deviation.

<i>Dependent variable:</i>	
Log Irrigated Surface	
a_0	0.112*** (0.024)
a_1	-0.051*** (0.009)
Observations	14058
Effects	County & Year
<i>Note:</i>	*p<0.1; **p<0.05; ***p<0.01

Table 6: Irrigation surface quadratic regression results

B Theory appendix

B.1 Properties of A

Proposition 6 *The function $A(\iota, \epsilon)$ defined in Equation (32) satisfies properties (A1), (A2) and (A3).*

Proof:

$$\frac{\partial A}{\partial \epsilon} = -\alpha \left[1 - \underbrace{\frac{\iota^\kappa}{\theta} e^{-h\epsilon}}_{\leq 1} (1 - \epsilon h) \right] < 0$$

Which shows (A1).

For a set ϵ , the function A is constant by part on the domain where $\frac{\iota^\kappa}{\theta} e^{-h\epsilon}$ would be greater than 1. This does not prevent the regularity of the overall objective as the expectation over all values of ϵ with probability greater than 0 will make sure that the overall objective is strictly concave (as some of the components of the sum will be strictly concave and others constant, the expectation is a strictly concave

function. We take the first order derivative on the interval where the function is not constant:

$$\frac{\partial A}{\partial \iota} = \alpha \epsilon \kappa \frac{\iota^{\kappa-1}}{\theta} e^{-h\epsilon} > 0$$

And the second order derivative:

$$\frac{\partial^2 A}{\partial \iota^2} = \alpha \epsilon \kappa (\kappa - 1) \frac{\iota^{\kappa-2}}{\theta} e^{-h\epsilon} < 0$$

which is negative because $\kappa < 1$. This shows (A2). Finally notice that the function $\epsilon e^{-h\epsilon}$ is increasing then decreasing with a maximum reached in $\bar{\epsilon} = \frac{1}{h}$, proving (A3).

B.2 Section 3.1

Proof of Proposition 2: Equivalence between (2) and (3) is trivial as a is the derivative of S with respect to d . The marginal product of irrigation investment writes:

$$\frac{1}{\bar{y}} \frac{\partial y}{\partial \iota} = R(d) - \bar{p} - c_j(d) \iota^\xi \quad (42)$$

Given that $c(d)$ is weakly increasing in d by assumption, we have that if $\frac{1}{c(d)} \frac{\partial y}{\partial \iota}$ is increasing in d , then $\frac{\partial y}{\partial \iota}$ is increasing in d . Now notice that:

$$\frac{1}{c(d)} \frac{\partial y}{\partial \iota} = \frac{R(d) - \bar{p}}{c_j(d)} - \iota^\xi$$

The first term on the left-hand side is exactly the same as the term that depends on d in S_{it} . Hence when S_{it} is increasing in d , the quantity above is and therefore $\frac{\partial y}{\partial \iota}$ has to be increasing in d .

Then as $R(d)$ is monotonic bounded and $c(d)$ diverges by assumption, $\frac{\partial y}{\partial \iota}$ has to turn decreasing in d for d large enough, which shows that returns to irrigation investment are hump shaped with respect to d .

B.3 Macroeconomic Model Solution

Let us note $\psi(\epsilon)$ the pdf of ϵ and $\Psi(\epsilon)$ its cdf.

First we have the budget constraint in period 0 which allows to replace c_0 in the utility function:

$$y = c_0 + K + \iota \quad (43)$$

Assume first that $\iota > 0$. The Euler equation with respect to K writes:

$$(y_0 - \iota^* - K^*)^{-\gamma} = \beta \mathbb{E} \left(A(\epsilon, \iota^*)^{1-\gamma} (K^*)^{-\gamma} \right)$$

$$\frac{K^*}{y_0 - \iota^* - K^*} = \beta^{1/\gamma} \left(\int A(\epsilon, \iota^*)^{1-\gamma} \psi(\epsilon) d\epsilon \right)^{1/\gamma} \quad (44)$$

The Euler equation with respect to ι yields:

$$(y_0 - \iota^* - K^*)^{-\gamma} = \beta \mathbb{E} \left(A(\epsilon, \iota^*)^{-\gamma} (K^*)^{1-\gamma} \frac{\partial A}{\partial \iota} \right)$$

Re-organizing:

$$\left(\int A(\epsilon, \iota^*)^{1-\gamma} \psi(\epsilon) d\epsilon \right) = K^* \mathbb{E} \left(A(\epsilon, \iota^*)^{-\gamma} \frac{\partial A}{\partial \iota} \right) \quad (45)$$

Which gives us a full system of three equations for three unknowns. There are two corners to consider. The first one is of $\iota^* = 0$. This corner is never met as the marginal product of ι^* in 0 is positive infinity. The second corner to consider is when the derivative becomes flat because we have successfully mitigated all damages, i.e. :

$$\iota^\kappa \geq \theta e^{h\epsilon} \text{ for all possible } \epsilon \quad (46)$$

Then as all values above this threshold value deliver the same payoff, it is obviously wasteful to spend more than the threshold value itself. As a consequence the equilibrium sets:

$$\iota^\kappa = \theta e^{h\bar{\epsilon}} \quad (47)$$

where $\bar{\epsilon}$ is the maximum of the support of $\psi(\epsilon)$.

Deterministic solution In the deterministic case, the objective is not strictly concave and we will have several cases. If the solution is interior, then we obtain:

$$\begin{aligned} \frac{K^*}{y_0 - \iota^* - K_*} &= \beta^{1/\gamma} A^{\frac{1-\gamma}{\gamma}} \\ \iota^* \beta^{1/\gamma} A^{\frac{1-\gamma}{\gamma}} &= y_0 \times \beta^{1/\gamma} A^{\frac{1-\gamma}{\gamma}} - K^*(1 + \beta^{1/\gamma} A^{\frac{1-\gamma}{\gamma}}) \\ \iota^* &= y_0 - K^* \frac{1 + \beta^{1/\gamma} A^{\frac{1-\gamma}{\gamma}}}{\beta^{1/\gamma} A^{\frac{1-\gamma}{\gamma}}} \\ K^* &= \frac{1}{\theta} \frac{\epsilon \alpha \kappa \iota^{\kappa-1} e^{-h\epsilon}}{A} \\ \iota^* &= y_0 - \frac{1}{\theta} \frac{\epsilon \alpha \kappa \iota^{\kappa-1} e^{-h\epsilon}}{A} \frac{1 + \beta^{1/\gamma} A^{\frac{1-\gamma}{\gamma}}}{\beta^{1/\gamma} A^{\frac{1-\gamma}{\gamma}}} \end{aligned}$$

We can in particular take the comparative static of this quantity with respect to ϵ from the above expression. The function on the right hand side can be expressed as a strictly increasing function of the humped-shaped function $\epsilon e^{-h\epsilon}$, implying the same for ι .

Calculating expected damages Note $\frac{\iota^\kappa}{\theta} = b$ for the sake of notations. In the case where damages are non deterministic, the expected adaptation function writes:

$$\begin{aligned} 1 - \alpha \int_{\epsilon} \epsilon \min(1 - b e^{-h\epsilon}, 0) \phi(\epsilon) d\epsilon &= 1 - \alpha \int_{\frac{\log(b)}{h}}^{\infty} \epsilon (1 - b e^{-h\epsilon}) \phi(\epsilon) d\epsilon \\ 1 - \alpha \int_{\epsilon} \epsilon \min(1 - b e^{-h\epsilon}, 0) \phi(\epsilon) d\epsilon &= 1 - \alpha \mathbb{E}(\epsilon \mathbb{1}\{\epsilon \geq \frac{\log(b)}{h}\}) + \alpha b \int_{\log(b)/h}^{\infty} \epsilon e^{-h\epsilon} \phi(\epsilon) d\epsilon \end{aligned}$$

The second term has an immediate closed form due to the normal distribution:

$$\mathbb{E}(\epsilon \mathbb{1}\{\epsilon \geq \frac{\log(b)}{h}\}) = \mu + \frac{\psi(\frac{\log(b)}{h})}{1 - \Psi(\frac{\log(b)}{h})} \sigma^2$$

Now we handle the third term:

$$\begin{aligned} \int_{\log(b)/h}^{\infty} \epsilon e^{-h\epsilon} \phi(\epsilon) d\epsilon &= \frac{1}{\sqrt{2\pi}} \int_{\log(b)/h}^{\infty} \epsilon e^{-h\epsilon - (\frac{\epsilon-\mu}{\sigma})^2} d\epsilon \\ \int_{\log(b)/h}^{\infty} \epsilon e^{-h\epsilon} \phi(\epsilon) d\epsilon &= \frac{1}{\sqrt{2\pi}} \int_{\log(b)/h}^{\infty} \epsilon e^{-h\epsilon - (\frac{\epsilon-\mu}{\sigma})^2} d\epsilon \end{aligned}$$

B.4 Illustrations

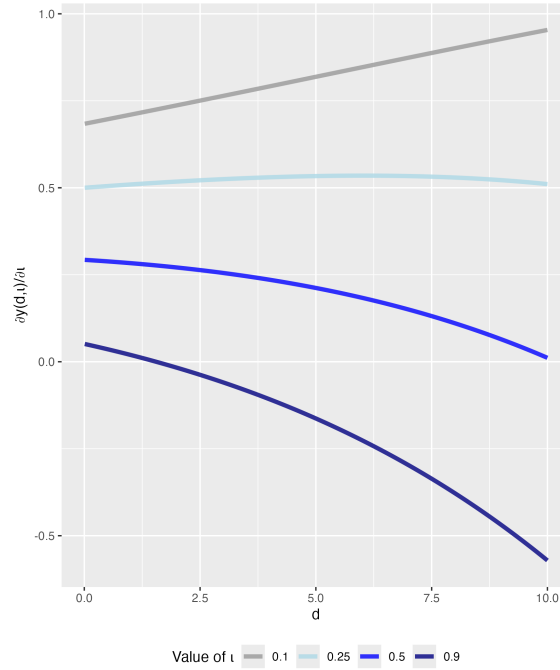


Figure 8: Marginal product of irrigation investment for different levels of irrigation investment and dryness

Values on Figure 8 correspond to a marginal product of investment given by Equation (42) with $R(d) - \bar{p} = e^{0.054d}$, $\xi = 0.5$ and $c(d) = e^{0.088d}$. The values 0.054 and 0.088 are taken from the values of coefficients b_1 and b_3 in Table 4 interpreted through the lens of Equation (13). These values are chosen arbitrarily for illustration purposes and do not constitute rigorous calibration.

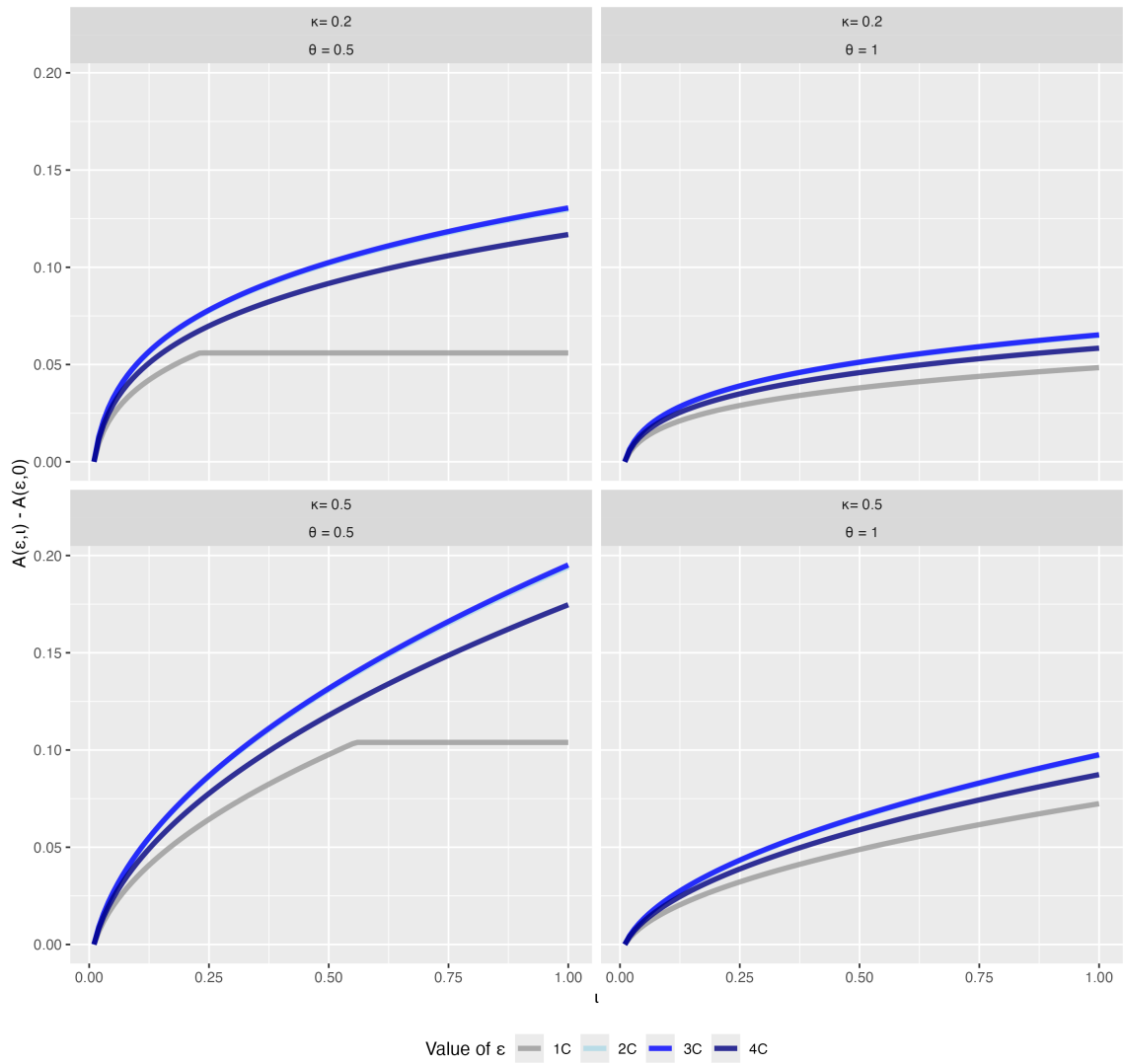


Figure 9: Total output saved by adaptation for different values of κ and θ